Clim Dyn (2014) 43:1001–1010
DOI 10.1007/s00382-013-1990-7

The role of sea ice in the temperature-precipitation feedback of glacial cycles

Hezi Gildor · Yosef Ashkenazy · Eli Tziperman · Ilit Lev

Received: 15 April 2013 / Accepted: 29 October 2013 / Published online: 10 November 2013

Abstract The response of the hydrological cycle to climate variability and change is a critical open question, where model reliability is still unsatisfactory, yet upon which past climate history can shed some light. Sea ice is a key player in the climate system and in the hydrological cycle, due to its strong albedo effect and its insulating effect on local evaporation and air-sea heat flux. Using an atmospheric general circulation model with specified sea surface temperature and sea-ice distribution, the role of sea ice in the hydrological cycle is investigated under last glacial maximum (LGM) and present day conditions, and by studying its contribution to the "temperature-precipitation feedback". By conducting a set of sensitivity experiments in which the albedo and thickness of the sea ice are varied, the various effects of sea ice in the hydrological cycle are isolated. It is demonstrated that for a cold LGM like state, a warmer climate (as a result of reduced sea-ice cover) leads to an increase in snow precipitation over the ice sheets. The insulating effect of the sea ice on the hydrological cycle is found to be larger than the albedo effect. These two effects interact in a nonlinear way and their total effect is not equal to summing their separate contribution.

Keywords Sea ice · Glacial-interglacial oscillations · Temperature-precipitation feedback · Hydrological cycle

H. Gildor (✉)
Institute of Earth Sciences, The Hebrew University of Jerusalem, Jerusalem 91904, Israel
e-mail: hezi.gildor@huji.ac.il

Y. Ashkenazy
Department of Solar Energy and Environmental Physics, The Blaustein Institutes for Desert Research, Ben-Gurion University of the Negev, Midreshet Ben-Gurion 84990, Israel

E. Tziperman
Department of Earth and Planetary Sciences, School of Engineering and Applied Sciences, Harvard University, Cambridge, MA, USA

I. Lev
Department of Environmental Sciences, Weizmann Institute of Science, Rehovot, Israel

1 Introduction

The expected response of the Earth's hydrological cycle and of land ice on future global warming has been the focus of many studies in recent years (Liu et al. 2009; Lambert and Webb 2008; Allan and Soden 2008; Allen and Ingram 2002; Cohen et al. 2012), yet modern observations and model results cannot conclusively predict this response. Studying past climate history and modeling of past climate improve our understanding of climate dynamics and may help to better understand this fundamental issue, eventually leading to better climate models. The aim of the present work is to study the role of sea ice in the hydrological cycle, focusing on rain and snow falling over the past (Last Glacial Maximum, LGM) major ice sheets.

Sea ice is a key player in the climate system, affecting local, and to some degree remote regions, via its albedo effect. Sea ice also strongly reduces air-sea heat and moisture fluxes (Ruddiman and McIntyre 1981; Gildor and Tziperman 2000), and thus may cause the air overlying it to be cooler and drier compare to air overlying ice-free ocean (Chiang and Bitz 2005). A significant part ($\sim$33 %) of the precipitation over the northern hemisphere (NH) ice sheets is believed to have originated locally from the Norwegian, Greenland and the Arctic seas (Charles et al. 1994;

Colleoni et al. 2011). Lastly, sea ice affects the location of the storm track and therefore indirectly also the patterns of precipitation (e.g. Laine et al. 2009; Li and Battisti 2008).

Its effect on the hydrological cycle makes sea ice a potentially significant player in the temperature-precipitation feedback (Le-Treut and Ghil 1983), according to which increase in temperature intensifies the hydrological cycle and thus the snow accumulation over ice sheets. This feedback is an important part of the sea-ice switch mechanism for glacial cycles, for example Gildor and Tziperman (2000). Indeed, proxy records show drastic increase in accumulation rate during interstadial periods (Cuffey and Clow 1997; Alley et al. 1993; Lorius et al. 1979), when the sea-ice retreats from its maximal extent.

Modeling studies of the response of the Antarctic ice sheet to greenhouse warming also suggest that for a temperature increase of up to 5.3 °C from present day temperatures, the increased accumulation still dominates the increase in ablation (Huybrechts and Oerlemans 1990). The Greenland ice sheet seems to be more sensitive to warming, but for glacial climate, the temperature-precipitation feedback is expected to be relevant (Huybrechts et al. 1991, Fig. 3). For warm climates, most precipitation falls as rain, and the temperature precipitation feedback does not result in increased snow accumulation (Tziperman and Gildor 2003; Gildor 2003). Although a few studies suggest that this feedback may be also relevant in the context of future warming due to CO_2 increase (Miller and de Vernal 1992; Ledley and Chu 1994), the threshold temperature allowing glaciers to grow due to increased temperature is not known.

Previous studies of the hydrological cycle during the LGM (Smith et al. 2003; Ramstein et al. 2005; Lohmann and Lorenz 2000; Charles et al. 1994; Vettoretti et al. 2000; Bromwich et al. 2005; Hofer et al. 2012), tested the effects of different boundary conditions, e.g., equatorial sea surface temperature (Lohmann and Lorenz 2000) or ice sheet topography (Felzer et al. 1996; Hakuba et al. 2012). While studying the Greenland $\delta^{18}O$ ice core variability, Charles et al. (1994) found four present-day main sources of precipitation over Greenland, in contrast with only two during the LGM. Expanded LGM sea-ice cover (including summer time) and cooler sea surface temperature, led to a smaller Norwegian-Greenland sea moisture source, illustrating the insulating effect of sea ice. In a related study, Smith et al. (2003) compared the effects of two estimates of sea-ice cover for the last glacial maximum (LGM) using the CCM3 model (Kiehl et al. 1998). They showed that snowfall over land ice decreases in a maximal sea-ice configuration compared to the minimal sea-ice configuration, and suggested that the source for the differences is the shifting of storm tracks southward.

While we also conduct experiments with different sea-ice extents, our main aim is to identify which of the climate feedbacks of sea ice is most effective in controlling snowfall rather than which geographical regions are responsible for the effect. Several sea-ice feedbacks are examined: albedo (and hence cooling), insulation that affects air sea heat and moisture fluxes, and the effect of sea ice on the storm track location. This is done using the National Center for Atmospheric Research (NCAR) Community Atmospheric General Circulation Model version 3.1 (CAM3, Holland et al. 2006), with specified sea surface temperature (SST) and sea ice. We conducted the following set of experiments,

1. Present day run (denoted "PD").
2. LGM run with a prescribed sea-ice, SST, orbital parameters and an estimated atmospheric greenhouse gas composition of 18 kyr ago (LGM).
3. LGM run but with sea-ice distribution as for the present day (PDSI).
4. LGM run but with sea-ice albedo set as open ocean albedo, to separate the albedo effect of sea ice from its insulation effect (SIalb).
5. LGM run without sea ice but with an albedo of sea ice over areas that sea ice exists during the LGM, to isolate the insulation effect of sea ice coverage (SIcov).

This set of experiments allows us to study each of the sea-ice feedbacks that influence the hydrological cycle (Table 1). We focus on rain and snow falling over the major NH high latitude ice sheets and over the storm track regions. We find that reducing the sea-ice extent under LGM conditions results in enhancement of the hydrological cycle, in accordance with the temperature-precipitation feedback. We also show that reducing the sea-ice albedo or eliminating the sea ice insulating effect by reducing its thickness to zero but keeping its albedo, both lead to increased precipitation and snow. However, surprisingly, the insulation of sea ice has a more pronounced effect on the hydrological cycle than the albedo. In summing up these changes, we found that they are not linear.

These sensitivity tests demonstrate the importance of the temperature-precipitation feedback, due to sea ice effects, in the growing process of ice sheets. For a sufficiently cold climate, e.g., under LGM conditions, reducing the extent, albedo, or insulating effect of sea ice, leads to increase in temperature and snow accumulation.

This paper is organized as followed: In Sect. 2 we briefly describe the model and compare the full LGM setup run to previous studies. The results of the sensitivity experiments are presented in Sect. 3, followed by a discussion in Sect. 4.

Table 1 Precipitation and snow (in parentheses) in mm yr^{-1} for the present-day experiment (PD), LGM, LGM with present-day sea ice (PDSI), LGM with sea-ice albedo equal albedo of sea (SIalb), and LGM but without the insulating effect of sea ice (SIcov)

Experiment	PD	LGM	PDSI	SIalb	SIcov
Global	1,030 (56)	908 (102)	918 (107)	911 (103)	912 (104)
Over Laurentide	704 (194)	389 (272)	431 (307)	399 (280)	411 (290)
Over Greenland	527 (273)	209 (137)	288 (231)	218 (176)	258 (204)
Over Fenno-Scandinavian	765 (137)	452 (329)	500 (360)	459 (333)	486 (349)

2 Model description

We used the National Center for Atmospheric Research (NCAR) Community Atmospheric Model version 3.1 (CAM3), at a T42 resolution ($\approx 2.875°$) and with 26 sigma-hybrid vertical levels (Holland et al. 2006). This model has been extensively used for present day (PD) (Collins et al. 2006; Hurrell et al. 2006; Hack et al. 2006) and past climate (e.g., Otto-Bliesner et al. 2006) research. The SST and sea-ice fraction are prescribed in all experiments. The sea ice thickness is kept constant during the runs at 2 m for the Northern Hemisphere and 1 m for the Southern Hemisphere. We set the open water albedo to 0.06, the sea-ice albedo to 0.68 for visible wavelength range and 0.3 for near infrared (NIR) wavelength respectively; the snow albedo depends on the snow's thickness, with a maximal albedo of 0.95 and 0.7 for visible and NIR wavelength ranges. Since the sea ice is kept constant in all runs we assume the surface albedo also remain constant throughout the run (ignoring possible effects due to snow accumulation over sea ice).

For the LGM experiments, seasonal sea-ice extent and SST are prescribed based on a fully coupled CCSM run with LGM boundary conditions (Otto-Bliesner et al. 2006) and surface elevation and ice sheet extent based on ICE-5G (Peltier 2004). Appropriate LGM values are used for orbital parameters, land mask changes due to sea level drop, and atmospheric greenhouse gas concentrations (Monnin et al. 2001; Dallenbach et al. 2000): CO_2, CH_4 and N_2O are set to 185 ppm, 350 and 200 ppb, respectively compared with 355, 1,714, and 311 for PD simulation. Sulfate aerosols, ozone and vegetation are set to pre-industrial conditions, following the Paleoclimate Modeling Inter-comparison Project (PMIP-2) protocol.

All model experiments were run for 20 years; shown averages and standard deviation are based on last the 10 years of simulation.

3 Results

3.1 Full LGM simulation

The global, annual mean surface air temperature (SAT) of the full LGM run is 7.8, 6.6 °C lower than the PD mean and within the range of 4.3–10.1 °C that was reported in previous studies (Bush and Philander 1999; Kim et al. 2008; Kim et al. 2003; Webb et al. 1997); the zonal annual mean SAT is similar to that of Otto-Bliesner et al. (2006).

The global average total precipitation (including both liquid and solid phases, hereafter referred to as 'precipitation') during LGM is 908 mm yr^{-1} (similar to Otto-Bliesner et al. 2006; Hall et al. 1996), a decrease of 11 % compared to PD. Like in previous studies (Broccoli and Manabe 1987; Hall et al. 1996; Otto-Bliesner et al. 2006; Bush and Philander 1999; Kim et al. 2003) the model's LGM climate is drier than PD. The global distribution of the December–January–February (DJF) precipitation is shown in Fig. 1. The tropical precipitation belt moves southward during the LGM, with a decrease in precipitation. Similarly, precipitation patterns between 30° and 45°N, over the north Pacific and north Atlantic move equatorward during the LGM, and become more confined in the meridional direction. In terms of seasonality, the maximal precipitation in the NH appears in September at LGM and in November at PD, and the minimum is in March at LGM and in April today (not shown).

The amount of snow increases by 46 mm yr^{-1}, an increase of 82 % compared to PD, much more dramatic than corresponding changes in total precipitation, with a global mean of 102 mm yr^{-1}. The snow precipitation maxima are located over the North Atlantic and the Norwegian Sea, over south Alaska and northwest Canada, south Canada and the Bering Sea (Fig. 2). Hall et al. (1996) already noted that a greater percentage of precipitation falls as snow during LGM compared to PD. This is especially pronounced over areas that were occupied by ice during LGM, over which 69 % of the total precipitation is snow in the LGM run and only 36 % is snow in the PD model run. When focusing on the three major ice sheets of the LGM, the model produces more snow precipitation in the LGM run over the Laurentide and the Fenno-Scandinavian ice sheets, and less over Greenland (changes of 40, 140 and −60 % respectively). Over the Laurentide ice sheet, summer snow is as intensive as in winter, but falls over higher latitudes (Fig. 3). In Greenland, however, snow mainly falls during summer, covering south-eastern Greenland. During winter the snow falls over the southern

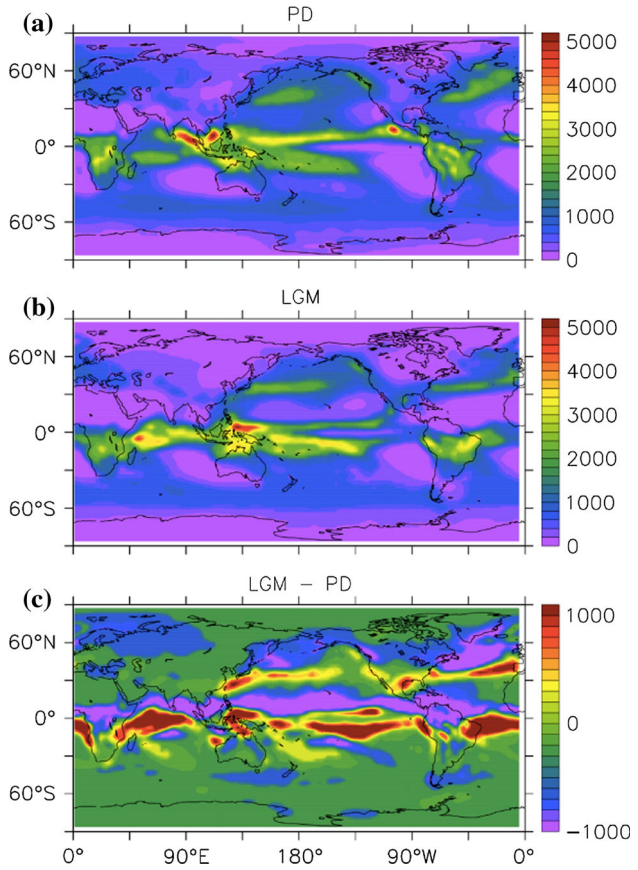

Fig. 1 Distribution of December–January–February (DJF) total precipitation (rain and snow) in [mm yr^{-1}] at **a** Present-day (PD), **b** Last Glacial Maximum (LGM), and **c** LGM minus PD

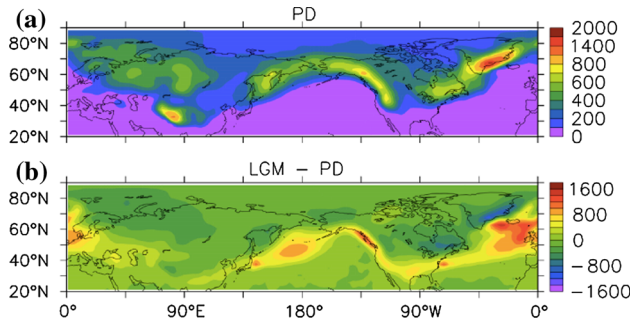

Fig. 2 December–January–February (DJF) snow rate [mm yr^{-1}] at **a** Present-day (PD), and **b** Last Glacial Maximum (LGM) minus PD

tip of Greenland and southward at a significantly larger amplitude (Fig. 3).

The model LGM jet stream and the associated storm track, appear 3° south of their present position, which mean that more precipitation fall at the southern edge of the ice sheets and southward from there. We diagnose the storm tracks using the atmospheric eddy kinetic energy (1) at 250 hPa (level of the jet stream maximum),

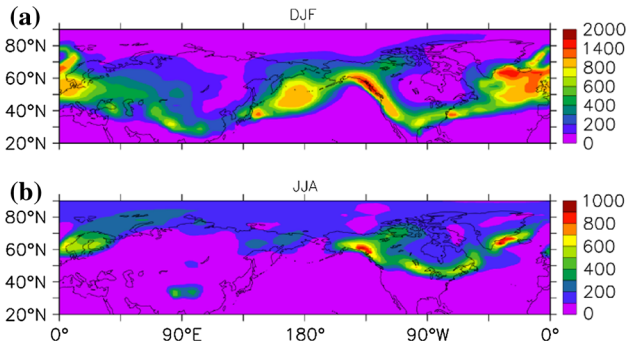

Fig. 3 Last glacial maximum (LGM) mean snow rate [mm yr^{-1}] for **a** December–January–February (DJF) and **b** June–July–August (JJA)

$$\frac{1}{2}\left(\overline{u'u'} + \overline{v'v'}\right), \tag{1}$$

where overbar denotes time average and the primes indicate daily fields. The eddy kinetic energy is shown together with the jet stream and the total precipitation (Figs. 4, 5). During the LGM, the jet seems to be more meridionally confined. Consistent with the storm tracks and the jets, the precipitation regions also migrate southward and become narrower.

3.2 LGM with PD sea ice

Model run PDSI denotes an experiment using LGM conditions but with prescribed seasonal sea-ice cover of PD. The sea-ice configuration appears in Fig. 6. This experiment tests the direct effect of sea ice cover on snow accumulation over land ice sheets during glacial periods (an important part of the sea-ice switch glacial cycle mechanism of Gildor and Tziperman 2000; Gildor and Tziperman 2001; see also Smith et al. 2003). In this run the NH sea-ice covered area is only $\sim$46 % of that of the LGM run.

The climate in this experiment is warmer than the LGM run, by almost 2 °C, and slightly wetter, by $\sim$1 % in the annual mean precipitation rate and 5 % in the snow fall rate. Over Greenland the snow precipitation in PDSI exceeds LGM by 80 mm yr^{-1} (38 %), over the Fenno-Scandinavian ice sheet by 48 mm yr^{-1} (11 %), and over the Laurentide ice sheet by 42 mm yr^{-1} (11 %). The global annual snow rate, 107 mm yr^{-1}, increases in PDSI by 5 % from LGM and by 91 % from PD. The snowfall distribution is mostly similar to LGM, but over the north Atlantic it extends more to the west and reaches Newfoundland. The main local differences in the snow fall rate (Fig. 7) are over the north Atlantic and the north-west Pacific (areas covered by sea ice in the LGM run but not in PDSI).

Although the globally averaged difference between LGM and PDSI is not very large, most of the increases in both total precipitation and snow precipitation take place over the edge of the ice sheets. The greatest increase is over

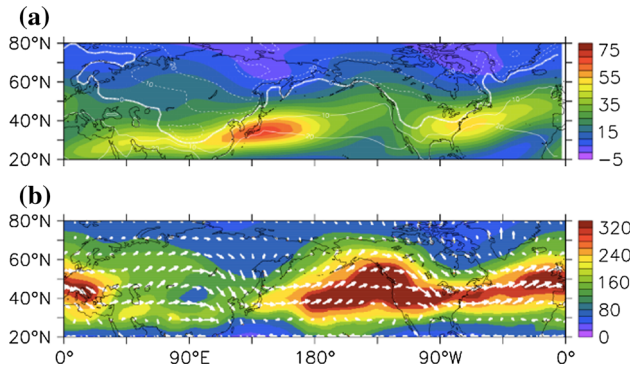

Fig. 4 Present-day winter model storm tracks: **a** the jet stream (zonal wind at ~250 hPa, [m s^{-1}]) with surface temperature contours [°C], **b** ~850 hPa wind vectors [m s^{-1}] and eddy kinetic energy contours [m^2 s^{-2}]

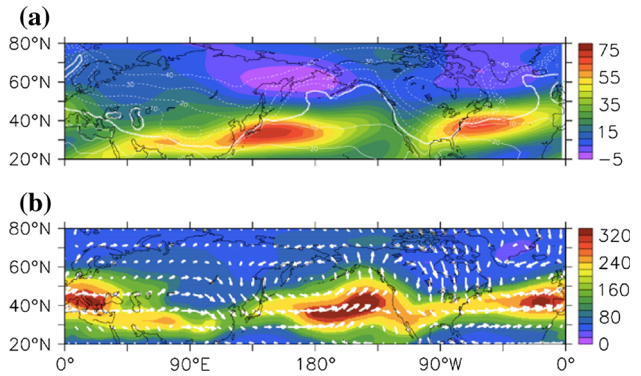

Fig. 5 Like Fig. 4 but for last glacial maximum (LGM)

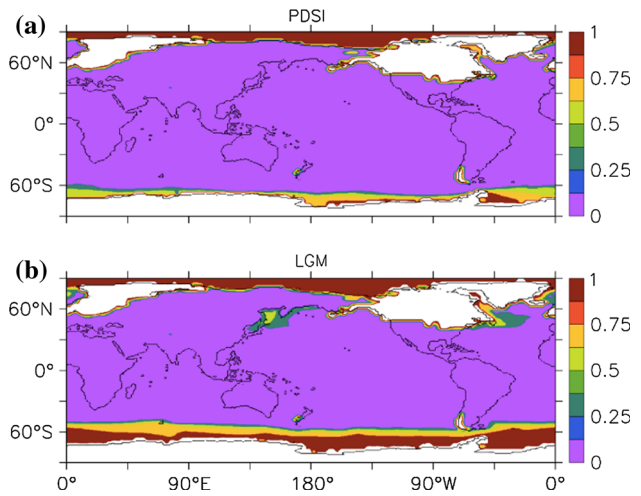

Fig. 6 Annual mean sea-ice fraction (between 0 and 1) and land ice (in *white*) for experiments **a** Present-day sea ice (PDSI) and **b** last glacial maximum (LGM)

Greenland with an increase of 38 % in the snowfall rate (to 231 mm yr^{-1}). Over the Laurentide ice sheet the increase is 13 % and over the Fenno-Scandinavian ice sheet, it is 9 %; these differences are significant as the error bars

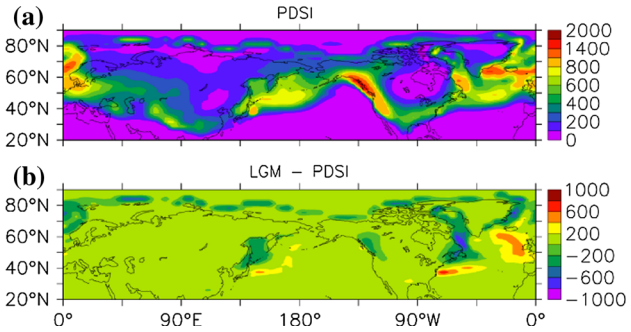

Fig. 7 December–January–February (DJF) snow rate [mm yr^{-1}] at **a** Present-day sea ice (PDSI) and **b** last glacial maximum (LGM) minus Present-day sea ice (PDSI)

(computed based on the interannual variability) are well separated (Fig. 8). This simulation resembles the sensitivity test performed by Smith et al. (2003), in which they compared the maximal and minimal sea-ice configurations of the LGM. We also found that snowfall rate is higher over ice sheets for the minimal sea-ice extent simulation (PDSI). However, unlike Smith et al. (2003), we found very small shifts in storm track location and storm intensity compared with LGM. The differences between LGM and PDSI in the locations of the storm tracks are much smaller than the differences between LGM and PD (with local maximal amplitude differences of 13–20 % in the distribution of eddy kinetic energy and the zonal wind at 250 hPa). Thus, in the runs reported here, the storm track is affected more by the continental ice sheets (because of their elevation) and the sea ice is of lower-order importance.

3.3 Sea-ice albedo effect

To isolate the effect of sea-ice albedo on climate, focusing, again, on precipitation over the ice sheets, we conducted a run with LGM conditions, but reducing the albedo of sea ice from 0.68 (visible) and 0.30 (NIR) to 0.06 for both wavelength bands, same albedo as open water. We thus take into account the insulating effect of sea ice but not its albedo effect in this run, and this run is accordingly denoted SIalb.

The SIalb climate is slightly warmer, by 0.65 °C, but has a similar annual global mean precipitation and snowfall rate compared to the full LGM run. Annual global mean precipitation is approximately 910 mm yr^{-1} (an increase of 0.3 % compared to the LGM experiment).

The global annual snow rate is also only 1 % higher than that of LGM, at 103 mm yr^{-1}. The snow-to-precipitation ratio is 11 %, and it is marginally higher than in the LGM run. Over Greenland there is an increase of 5 % in the snowfall rate (to 176 mm yr^{-1}), over the Laurentide ice sheet the increase is 3 %, and over the Fenno-Scandinavian

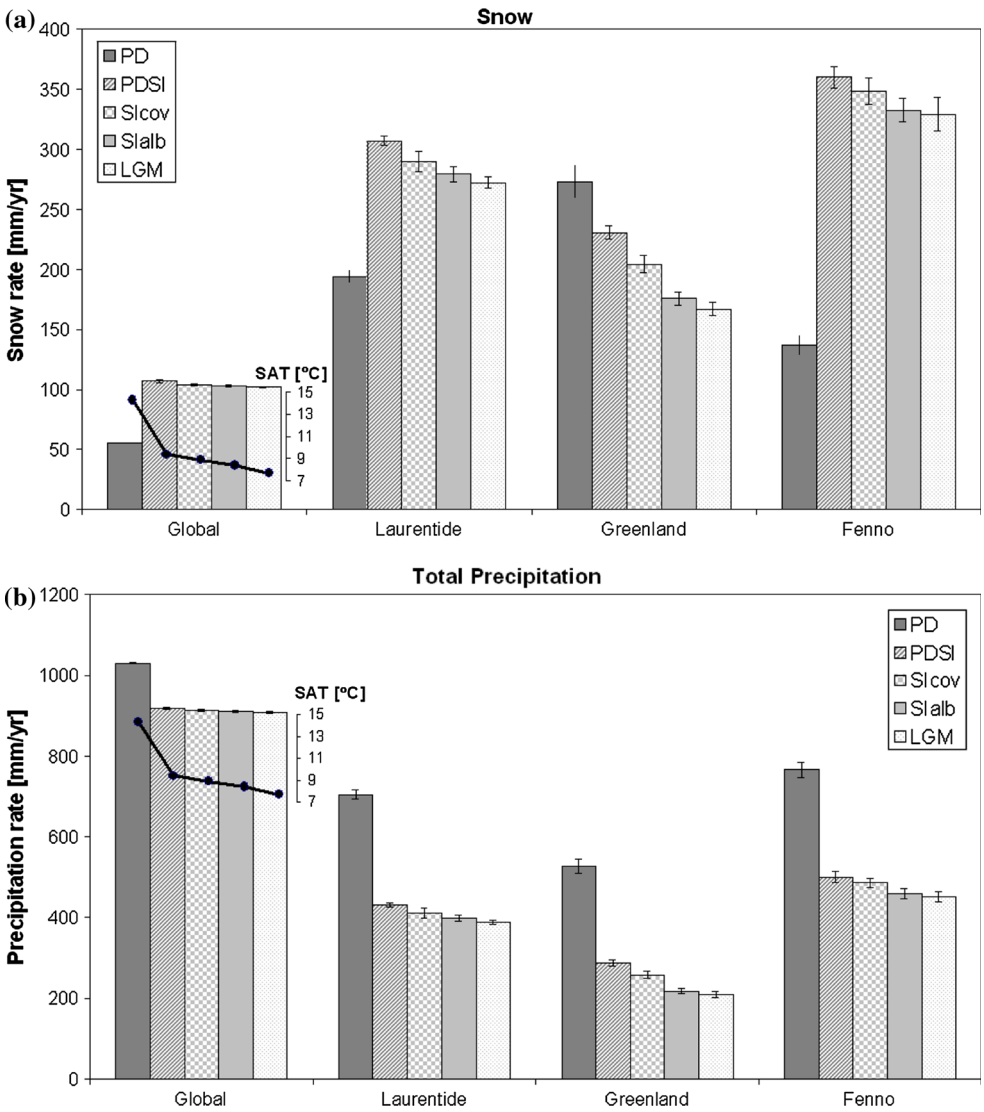

Fig. 8 Annual average of snow (**a**) and total precipitation (**b**) for the three major ice sheets and the global average, for the different experiments: Present day (PD); Last Glacial Maximum (LGM) but with present-day sea ice (PDSI); LGM with sea-ice thickness equals zero (SIcov); LGM with sea-ice albedo equals ocean albedo (SIalb); LGM. Also shown is the global mean surface air temperature (SAT). *Error bars* are based on the interannual variations

ice sheet the increase is only 1 %. The main differences in snowfall rates are more apparent during the summer months (JJA). These differences have a local magnitude of about 100 mm yr^{-1}. More snow falls in SIalb over the Arctic and the Baffin Bay, compared with LGM. Note that these regions are both covered by sea ice. The snowfall region at south Greenland is shifted slightly north in SIalb and covers a larger part of Greenland (Fig. 9).

3.4 Sea-ice insulating effect

The final experiment, termed SIcov, quantifies the insulating effect of sea ice by setting the sea-ice thickness to zero but keeping its albedo. Thus, the albedo effect of sea ice is active but other than that, sea ice behaves almost as open water, in particular, its insulating effect on air-sea fluxes is missing. Snow accumulation over sea ice is not possible (as over open water).

The SIcov solution is warmer in global average by 1.2 °C than LGM. Precipitation, snow rate, and snow-to-precipitation ratio are again very similar to those of LGM, but over land the differences are more apparent. Differences between winter snow in SIcov and LGM are shown in Fig. 10. More snow falls in SIcov relative to the LGM run over regions with sea ice, and mostly over the Baffin Bay, the Greenland Sea, and west Canada, whereas it is more snowy in the LGM run over the North Atlantic. Over Greenland there is an increase of 22 % in the snowfall rate; both over the Laurentide and the Fenno–Scandinavian ice sheets the increase is about 6 %.

The comparison of SIcov and SIalb makes it evident that sea-ice insulating effect has a greater effect on snowfall over land ice than the albedo. The control of snowfall over the three major ice sheets of the LGM by sea ice is of special interest, and we find that SIcov is more snowy there than SIalb (but less than PDSI, where both the insulation

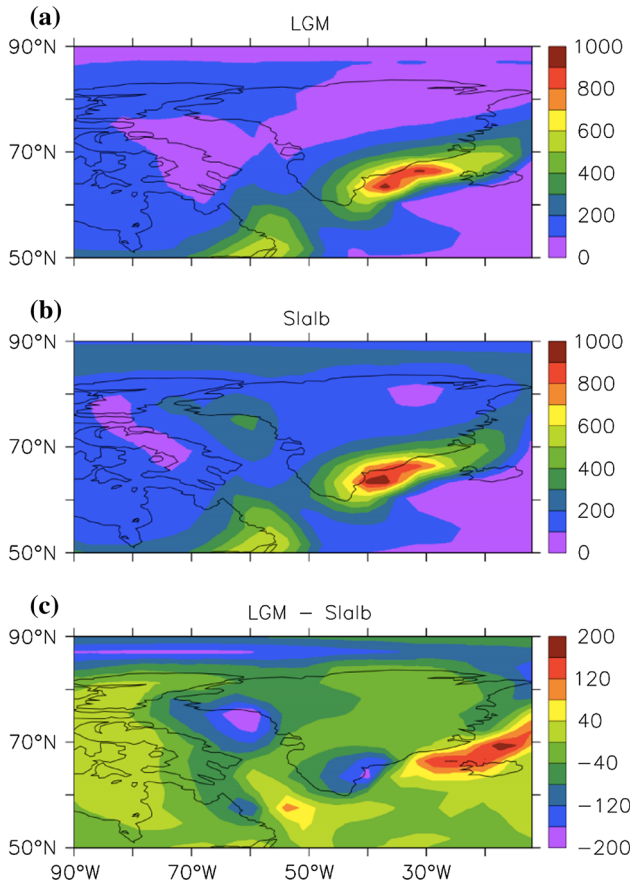

Fig. 9 June–July–August (JJA) snow rate [mm yr^{-1}], with zoom over Greenland, at **a** LGM, **b** SIalb, and **c** LGM minus SIalb

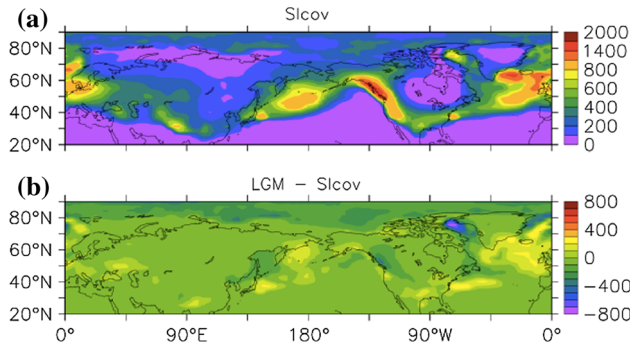

Fig. 10 December–January–February (DJF) snow rate [mm yr^{-1}] at **a** SIcov and **b** LGM minus SIcov

and albedo effects are eliminated). Thus the sea-ice cover has a greater effect on snowfall over land ice than the albedo has.

3.5 Nonlinear interaction effect

It is interesting to check whether the different effects of sea ice can be linearly superimposed or whether there is a nonlinear feedback between them. For this purpose we define an index, I_v, as follows. Let v a variable such as snowfall rate, precipitation rate, temperature, etc. Then $(v_{\mathrm{SIalb}} - v_{\mathrm{PDSI}})$ is the effect of the insulation feedback of sea ice only on v. Similarly, $(v_{\mathrm{SIcov}} - v_{\mathrm{PDSI}})$ is the effect of the albedo feedback only. Run PDSI lacks both the albedo and insulating effects. If the albedo effect and the insulating effect can be summed linearly, their addition is supposed to be equal to the PDSI simulation (in the PDSI we reduce the sea-ice extent, and summing SIalb and SIcov reduces the extent in two stages: first reducing the albedo and then the covering effect). Eventually, one expects that when all experiments are added, one obtains the same snowfall/precipitation/temperature as in LGM experiment. Define therefore the following index,

$$I_v = (v_{\mathrm{SIalb}} - v_{\mathrm{PDSI}}) + (v_{\mathrm{SIcov}} - v_{\mathrm{PDSI}}) + v_{\mathrm{PDSI}} - v_{\mathrm{LGM}} = v_{\mathrm{SIalb}} + v_{\mathrm{SIcov}} - v_{\mathrm{PDSI}} - v_{\mathrm{LGM}}. \quad (2)$$

If climate response to the sea ice feedbacks were linear, this index should vanish.

We calculated the indices of precipitation, snow, and surface temperatures for the sea-ice effects (a NH distribution of the indices is shown in Fig. 11). Note that the index units are the same as the chosen variables. The indices do not show any defined trend, and the values over ice sheets vary dramatically between positive and negative

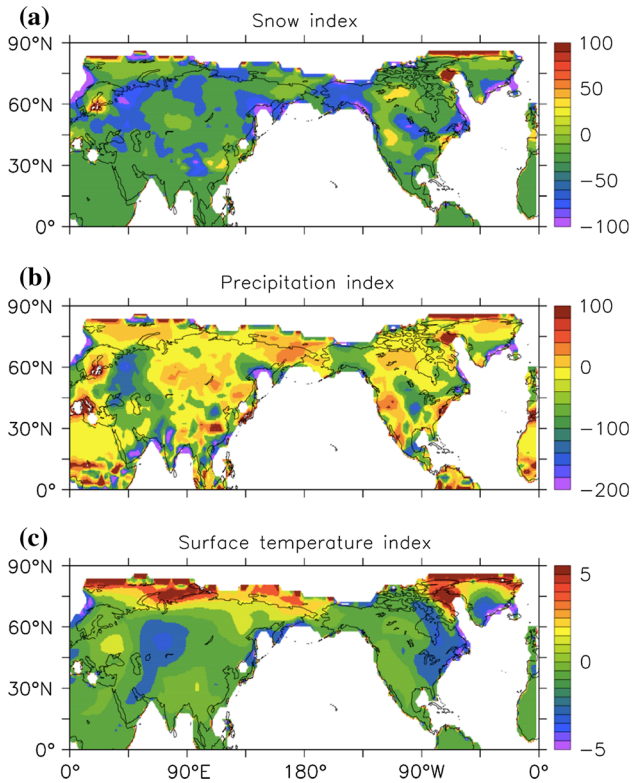

Fig. 11 Sea ice effects index I_v calculated for **a** snow [mm yr^{-1}], **b** precipitation [mm yr^{-1}], and **c** surface temperature [°C]

values, showing that the effects are not linear. Global averages of the indices are -2.2 mm yr^{-1} for snow, -2.7 mm yr^{-1} for precipitation, and 0.1° for surface temperature. From the global means we found that eliminating the sea ice has a greater influence on precipitation than summing both sea-ice albedo and cover reduction, indicating an interesting nonlinear feedback effect that will be investigated in future study.

4 Discussion

In this work we studied the role of sea ice in the hydrological cycle during the LGM, and in particular examined sea ice feedbacks responsible for the temperature-precipitation feedback according to which a warming anomaly to a cold, LGM-like, climate leads to enhanced snow accumulation rate over land ice sheets. This temperature-precipitation feedback where a warming anomaly leads to enhanced snow accumulation rates over land ice sheets in a cold LGM-like climate is a central component in several theories of glacial cycles (Källén et al. 1979; Le-Treut and Ghil 1983; Ghil et al. 1987; Ghil 1994; Gildor and Tziperman 2000, 2001; Tziperman and Gildor 2003). However, it should be noted that while we focused on the various effects of sea ice on precipitation, we did not run a full surface mass model of the ice sheets and we neglected the effects on ice ablation.

We performed three model experiments with LGM ice sheets and atmospheric composition to evaluate the contribution of sea-ice extent, sea-ice albedo, and sea-ice insulation effect on snowfall rates during the LGM. Overall, our results support the temperature-precipitation feedback. Total precipitation (rain plus snow) and snowfall rate, globally and over the three major LGM ice sheets, are summarized for the various experiments in Fig. 8 and Table 1. The global mean surface air temperature is also shown in Fig. 8.

Each of the experiments resulted in a temperature rise compared to the full LGM experiment, yet was still colder than the PD model experiment. We find that in a *cold, glacial climate* snowfall rate over the ice sheets is reduced as a result of increasing sea-ice extent (compare LGM and PDSI experiments). An increased sea-ice extent cools the climate even more, the precipitation belt is pushed southward and the hydrological cycle weakens. The main novel result here has to do with the identification of physical feedbacks by which the sea ice affects precipitation. We find that the albedo feedback of an extended sea-ice cover in an LGM-like climate only weakly affects the reduction of snowfall rate. For example, the snowfall over the Laurentide ice sheet in experiment LGM is 272 mm/yr, while when the sea ice is reduced to present-day extent, it is 307 mm/yr. That is, the sea ice suppresses the snowfall rate by a significant amount of 11 %. Run SIalb in which the sea ice is as in LGM, but its albedo effect is eliminated, shows a similar suppression relative to PDSI, to 280 mm/yr (9 %), indicating that the suppression of precipitation is not obtained via the albedo feedback of sea ice.

The other major feedback of sea ice is its insulating effect. Run SIcov shows a significantly weaker suppression from PDSI, from 307 to 290 (5 %), indicating that the insulating feedback is responsible for a large part of the suppression of precipitation by sea ice. It follows that the hydrological cycle is more sensitive to the insulating effect of sea ice than to its albedo. There are two reasons to the larger contribution of the insulating effect to the temperature-precipitation feedback. First, the overall cooling of the insulating effect is about twice than that of the albedo. This by itself is expected to lead to a more significant change in precipitation. In addition, the insulation effect not only reduce air-sea heat flux, it also directly prevents evaporation from ice-covered regions, which are a major source of precipitation over the NH ice sheets (Charles et al. 1994).

In all experiments, the region that is most sensitive to changes (in the sense of snow and precipitation) is Greenland. Sea-ice insulation also has a greater effect on temperature. The global mean surface temperature difference between LGM and SIcov is twice the difference between LGM and SIalb. These experiments as a whole indicate that in a cold, LGM-like climate, sea ice indeed suppresses snow accumulation over ice sheets (Gildor and Tziperman 2000). Clearly this is not the case in a warmer (PD) climate, when accumulation increases even more, but as rain rather than snow. Therefore, the temperature-precipitation feedback applies for a finite range of temperatures (Gildor 2003).

Overall, the area-averaged differences in snowfall rate are not very large, and are largest over Greenland (see also Li et al. 2005, 2010; Kiefer et al. 2002, in the context of Dansgaard-Oeschger cycles). However, as seen in Fig. 2, the differences are not evenly distributed and can be quite large in certain regions, mainly at the periphery of the ice-sheets. These regions are characterized by large thermal gradients due to the albedo differences between the ice and the adjacent land (Bromwich et al. 2005). The starvation of the ice sheets at their periphery by the presence of sea ice can stimulate their gradual withdrawal, followed by amplification by other feedbacks (land ice albedo, etc).

Future plans include analysis of the moisture transport in the different simulations, focusing on each of the three major ice sheets. We want to find the main sources of precipitation over each ice sheet, so we can conclude how different sea ice extents and covers affect the growth of land ice. It is also interesting to study the effect of southern

hemisphere sea ice on the NH high latitude hydrological cycle (teleconnection).

Acknowledgments This work was supported by the Israel-US Binational Science foundation. We thank Cecilia Bitz for providing the data for the LGM simulations. We thank Nili Harnik, Erick Fredj, Jeff Shaman, and Emmanuel Boss for helpful discussions and suggestions. ET is supported by NSF climate dynamics, P2C2 Grant ATM-0902844, and thanks to the Weizmann institute for its hospitality during parts of this work.

References

Allan RP, Soden BJ (2008) Atmospheric warming and the amplification of precipitation extremes. Science 321:1481–1484. doi:10.1126/science.1160787

Allen M, Ingram W (2002) Constraints on future changes in climate and the hydrologic cycle. Nature 419:224–232. doi:10.1038/nature01092

Alley RB, Meese D, Shuman C, Gow AJ, Taylor K, Grootes P, White J, Ram M, Waddington ED, Mayewski P, Zielinski G (1993) Abrupt increase in Greenland snow accumulation at the end of the Younger Dryas event. Nature 362:527–529

Broccoli AJ, Manabe S (1987) The influence of continental ice, atmospheric CO_2, and land albedo on the climate of the last glacial maximum. Clim Dyn 1:87–99

Bromwich DH, Toracinta ER, Oglesby RJ, Fastook JL, Hughes TJ (2005) LGM summer climate on the southern margin of the Laurentide Ice Sheet: wet or dry? J Clim 18:3317–3338

Bush ABG, Philander SGH (1999) The climate of the last glacial maximum: results from a coupled atmosphere-ocean general circulation model. J Geophys Res 104:24509–24525

Charles CD, Rind D, Jouzel J, Koster RD, Fairbanks RG (1994) Glacial-interglacial changes in moisture sources for Greenland: influences on the ice core record of climate. Science 263:508–511

Chiang JCH, Bitz CM (2005) Influence of high latitude ice cover on the marine intertropical convergence zone. Clim Dyn 25(5):477–496

Cohen JL, Furtado JC, Barlow MA, Alexeev VA, Cherry JE (2012) Arctic warming, increasing snow cover and widespread boreal winter cooling. Environ Res Lett 7(1):014,007. doi:10.1088/1748-9326/7/1/014007

Colleoni F, Liakka J, Krinner G, Jakobsson M, Masina S, Peyaud V (2011) The sensitivity of the Late Saalian (140 ka) and LGM (21 ka) Eurasian ice sheets to sea surface conditions. Clim Dyn 37(3–4):531–553. doi:10.1007/s00382-010-0870-7

Collins W, Bitz CM, Blackmon M, Bonan GB, Bretherton CS, Carton JA, Chang P, Doney S, Hack JJ, Henderson T, Kiehl JT, Large WG, McKenna D, Santer BD, Smith R (2006) The community climate system model, version 3. J Clim 19:2122–2143

Cuffey K, Clow G (1997) Temperature, accumulation, and ice sheet elevation in central Greenland through the last deglacial transition. J Geophys Res 102:26383–26396

Dallenbach A, Blunier T, Fluckiger J, Stauffer B, Chappellaz J, Raynaud D (2000) Changes in the atmospheric CH_4 gradient between Greenland and Antarctica during the Last Glacial and the transition to the Holocene. Geophys Res Lett 27:1005–1008

Felzer B, Oglesby R, Webb T, Hyman DE (1996) Sensitivity of a general circulation model to changes in northern hemisphere ice sheets. J Geophys Res 101:19077–19092

Ghil M (1994) Cryothermodynamics: the chaotic dynamics of paleoclimate. Physica D 77:130–159

Ghil M, Mullhaupt A, Pestiaux P (1987) Deep water formation and Quaternary glaciations. Clim Dyn 2:1–10

Gildor H (2003) When Earth's freezer door is left ajar. EOS 84(23):215

Gildor H, Tziperman E (2000) Sea ice as the glacial cycles climate switch: role of seasonal and orbital forcing. Paleoceanography 15:605–615

Gildor H, Tziperman E (2001) A sea-ice climate-switch mechanism for the 100 kyr glacial cycles. J Geophys Res 106:9117–9133

Hack JJ, Caron JM, Yeager SG, Oleson KW, Holland MM, Truesdale JE, Rasch PJ (2006) Simulation of the global hydrological cycle in the CCSM community atmosphere model version 3 (CAM3): mean features. J Clim 19:2199–2221

Hakuba MZ, Folini D, Wild M, Schaer C (2012) Impact of Greenland's topographic height on precipitation and snow accumulation in idealized simulations. J Geophys Res 117:D09,107. doi:10.1029/2011JD017052

Hall NMJ, Valdes PJ, Dong B (1996) The maintenance of the last great ice sheets: a UGAMP GCM study. J Clim 9:1004–1019

Hofer D, Raible CC, Dehnert A, Kuhlemann J (2012) The impact of different glacial boundary conditions on atmospheric dynamics and precipitation in the North Atlantic region. Clim Past 8(3):935–949. doi:10.5194/cp-8-935-2012

Holland MM, Bitz CM, Hunke EC, Lipscomb WH, Schramm JL (2006) Influence of the sea ice thickness distribution on polar climate in CCSM3. J Clim 19:2398–2414

Hurrell JW, Hack JJ, Phillips AS, Caron J, Yin J (2006) The dynamical simulation of the community atmosphere model version 3 (CAM3). J Clim 19:2162–2183

Huybrechts P, Oerlemans J (1990) Response of the Antarctic ice sheet to future greenhouse warming. Clim Dyn 5:93–102

Huybrechts P, Letreguilly A, Reeh N (1991) The Greenland ice sheet and greenhouse warming. Paleonogr Paleoclim Paleoecol 89:399–412

Källén E, Crafoord C, Ghil M (1979) Free oscillations in a climate model with ice-sheet dynamics. J Atmos Sci 36:2292–2303

Kiefer T, Lorenz S, Schulz M, Lohmann G, Sarnthein M, Elderfield H (2002) Response of precipitation over Greenland and the adjacent ocean to North Pacific warm spells during Dansgaard-Oeschger stadials. Terra Nova 14(4):295–300

Kiehl J, Hack J, Bonan G, Boville B, Williamson D, Rasch P (1998) The national center for atmospheric research community climate model: CCM3. J Clim 11:1311149

Kim SJ, Flato GM, Boer GJ (2003) A coupled climate model simulation of the last glacial maximum, part 2: approach to equilibrium. Clim Dyn 20(6):635–661

Kim SJ, Crowley TJ, Erickson DJ, Govindasamy B, Duffy PB, Lee BY (2008) High-resolution climate simulation of the last glacial maximum. Clim Dyn 31:1–16

Laine A, Kageyama M, Salas-melia D, Voldoire A, Riviere G, Ramstein G, Planton S, Tyteca S, Peterschmitt JY (2009) Northern hemisphere storm tracks during the last glacial maximum in the PMIP2 ocean-atmosphere coupled models: energetic study, seasonal cycle, precipitation. Clim Dyn 32:593–614

Lambert FH, Webb MJ (2008) Dependency of global mean precipitation on surface temperature. Geophys Res Lett 35. doi:10.1029/2008GL034838

Ledley TS, Chu SP (1994) Global warming and the growth of ice sheets. Clim Dyn 9:213–219

Le-Treut H, Ghil M (1983) Orbital forcing, climatic interactions, and glaciations cycles. J Geophys Res 88:5167–5190

Li C, Battisti D (2008) Reduced Atlantic storminess during last glacial maximum: evidence from a coupled climate model. J Clim 21(24):3561–3579

Li C, Battisti DS, Schrag DP, Tziperman E (2005) Abrupt climate shifts in Greenland due to displacements of the sea ice edge. Geophys Res Lett 32(19):L19,702. doi:10.1029/2005GL023492

Li C, Battisti DS, Bitz CM (2010) Can north Atlantic sea ice anomalies account for Dansgaard-Oeschger climate signals? J Clim 23(20):5457–5475. doi:10.1175/2010JCLI3409.1

Liu SC, Fu C, Shiu CJ, Chen JP, Wu F (2009) Temperature dependence of global precipitation extremes. Geophys Res Lett 36. doi:10.1029/2009GL040,218

Lohmann G, Lorenz S (2000) On the hydrological cycle under paleoclimatic conditions as derived from AGCM simulations. J Geophys Res 105:17417–17436

Lorius C, Merlivat L, Jouzel J, Pourchet M (1979) A 30,000-yr isotope climatic record from Antarctic ice. Nature 280:644–648

Miller G, de Vernal A (1992) Will greenhouse warming lead to Northern Hemisphere ice-sheet growth? Nature 355:244–246

Monnin E, Indermuhle A, Dallenbach A, Fluckiger J, Stauffer B, Stocker TF, Raynaud D, Barnola J (2001) Atmospheric CO_2 concentrations over the last glacial termination. Science 291:112–114

Otto-Bliesner BL, Brady EC, Clauzet G, Tomas R, Levis S, Kothavala Z (2006) Last glacial maximum and holocene climate in CCSM3. J Clim 19:2526–2544

Peltier WR (2004) Global glacial isostasy and the surface of the ice-age earth: the ICE-5G (VM2) Model and GRACE. Ann Rev Earth Planet Sci 32:111–149

Ramstein G, Khodri M, Donnadieu Y, Fluteau F, Godderis Y (2005) Impact of the hydrological cycle on past climate changes: three illustrations at different time scales. Comptes Rendus Geosci 337:125–137

Ruddiman WF, McIntyre A (1981) Oceanic mechanisms for amplification of the 23,000–year ice–volume cycle. Science 212:617–627

Smith LM, Miller GH, Otto-bliesner B, Shin SI (2003) Sensitivity of the northern hemisphere climate system to extreme changes in Holocene Arctic sea ice. Quat Sci Rev 22:645–658

Tziperman E, Gildor H (2003) The mid-Pleistocene climate transition and the source of asymmetry between glaciation and deglaciation times. Paleoceanography 18. doi:10.1029/2001PA000,627

Vettoretti G, peltier WR, McFarlane NA (2000) Global water balance and atmospheric water vapour transport at last glacial maximum: climate simulations with the Canadian climate centre for modelling and analysis atmospheric general circulation model. Can J Earth Sci 37:695–723

Webb RS, Rind DH, Lehman SJ, Healy RJ, Sigman D (1997) Influence of ocean heat transport on the climate of the last glacial maximum. Nature 385:695–699